

Energy scaling of a multipass-cavity mode-locked femtosecond bulk laser with a carbon nanotube saturable absorber

I. Baylam^a, S. Ozharar^b, H. Cankaya^a, S. Y. Choi^c, K. Kim^c, F. Rotermund^c, U. Griebner^d, V. Petrov^d, and A. Sennaroglu^{a*}

^aLaser Research Laboratory, Department of Physics, Department of Electrical-Electronics Engineering, Koç University Rumelifeneri, Sariyer, Istanbul, 34450, Turkey

^bCollege of Arts and Sciences, Bahcesehir University, Besiktas, Istanbul, 34353, Turkey

^cDepartment of Physics & Division of Energy Systems Research, Ajou University, 443-749 Suwon, Republic of Korea

^dMax Born Institute for Nonlinear Optics and Ultrafast Spectroscopy, 2A Max-Born-Str., 12489 Berlin, Germany

ABSTRACT

In the design of mode-locked lasers, single-walled carbon nanotube saturable absorbers (SWCNT-SAs) have emerged as important alternatives to semiconductor saturable absorber mirrors (SESAMs) due to their favorable optical characteristics, low cost, and relatively simple fabrication scheme. Therefore, it is of great interest to explore the limits of energy scaling in solid-state lasers mode-locked with SWCNT-SAs. Due to their unique wavelength range for biomedical applications, a room-temperature Cr⁴⁺:forsterite laser operating near 1.3 μm was used in the mode-locking experiments. The laser was end-pumped with a continuous-wave Yb-fiber laser at 1064 nm. Furthermore, a q-preserving multipass-cavity (MPC) was added to the short resonator to lower the pulse repetition rate to 4.51 MHz and to scale up the output pulse energy at low average power. The SWCNT-SA was fabricated with SWCNTs grown by the high-pressure CO conversion (HiPCO) technique. With dispersion compensation optics, the net group delay dispersion of the resonator was estimated to be around -4440 fs². When mode-locked with the SWCNT-SA, the resonator produced 10-nJ, 121-fs pulses at 1247 nm with a spectral bandwidth of 16 nm, corresponding to a time-bandwidth product of 0.37. To our knowledge, this represents the highest peak power (84 kW) generated to date from a bulk femtosecond solid-state laser, mode-locked by using a SWCNT-SA. The results also suggest that the peak power achieved in our experiments was limited only by the self-focusing in the Cr⁴⁺:forsterite gain medium and further increase in output energy should in principle be possible in other gain media mode-locked with SWCNT-SAs.

Keywords: Single walled carbon nanotube saturable absorber (SWCNT-SA), multipass-cavity (MPC), energy scaling, Cr⁴⁺:forsterite laser

1. INTRODUCTION

Due to their unique properties, carbon nanotubes (CNTs) have found new and diverse applications in both electronics and photonics. In particular, because of their fast recovery time (<2 ps) [1] and saturable absorption band in the near infrared, SWCNTs have been used as optical saturable absorbers for the mode-locking of numerous lasers [2-4]. Thanks to their broad optical bandwidth, simpler production, and lower cost, SWCNT-SAs have become important alternatives to widespread SESAMs [5]. In addition to these properties, the peak of the saturable absorption band can be changed by controlling the diameter distribution and the chirality of SWCNTs during the manufacturing stage. The chirality determines whether the CNT will act as metallic or semiconducting [6], and is defined by a pair of indices (n,m) of chiral vectors which determine the symmetry axis of the CNT in terms of unit cell vectors. The diameters of currently available SWCNTs are usually around 0.8-1.4 nm, which make them effective saturable absorbers for near-infrared mode-locked lasers. Therefore, it is of great interest to explore the limits of energy scaling in lasers mode-locked with SWCNT-SAs.

*asennar@ku.edu.tr; phone +90 212-338 14 00; fax 212-338-15 59

For this study, a room temperature Cr⁴⁺:forsterite gain medium operating around 1250 nm is chosen because of its potential biomedical applications. Due to Rayleigh scattering in biological tissue, short wavelengths have poor penetration, whereas wavelengths above 1.4 μm are strongly absorbed by water [7]. Therefore, the operation wavelength of the Cr⁴⁺:forsterite laser (1250 nm) is ideal for many biomedical applications that require deep tissue penetration such as multi-photon microscopy and optical coherence tomography [8, 9].

In order to explore the compatibility of SWCNT-SAs with high energy mode-locked lasers, we have built a Cr⁴⁺:forsterite resonator with a q-preserving multipass-cavity (MPC) extension [10]. With this resonator architecture, the fundamental cavity frequency was 4.51 MHz and the output pulse energy was scaled up to 10 nJ. To our knowledge, the corresponding peak power of 84 kW is the highest peak power ever obtained from a femtosecond solid-state laser mode-locked with a SWCNT-SA [11]. By using three different output couplers, the cavity nonlinearities that limit further energy scaling were also explored in the experiments.

2. EXPERIMENTAL SET-UP

2.1 Cr⁴⁺:forsterite laser set-up

The short x-cavity was constructed with two curved dispersion compensation mirrors (DCMs), each with 10 cm radius of curvature (RC) (M1, and M2), two flat folding mirrors (M3 and M4), two flat end mirrors (M5, and M10 as the output coupler), and a 20-mm-long Brewster-cut Cr⁴⁺:forsterite crystal as seen in Fig. 1. The crystal was mounted in a copper holder and maintained at a constant temperature of 20° by water cooling. The Cr⁴⁺:forsterite crystal with 70 % absorption at the pump wavelength was end pumped by a continuous wave (CW) Yb: fiber laser at 1064 nm. With this laser configuration, an average CW output power of 815 mW was obtained using a 4.7 % flat output coupler (OC) at a pump power of 8 W.

In order to create an intracavity beam waist for saturating the SWCNT-SA and to increase the group delay dispersion (GDD) of the cavity, the flat output coupler (M10) was removed and the cavity arm was further extended with DCMs and Gires-Tournois interferometer (GTI) mirrors. Each DCM (M13, M14, M19) and GTI (M11, M12, M17, M18) mirror had -150 fs² and -250 fs² of GDD, respectively. As seen from the schematic in Fig. 1, the optical path was aligned such that the beam reflected four times from each GTI mirror in each roundtrip to maximize the total negative dispersion. After accounting for the positive dispersion coming from the crystal (+800 fs²), MPC (+360 fs²), quartz substrate (+7 fs²), air (+794 fs²) and negative dispersion contributions of the other DCMs in the short x-cavity, and in the MPC (M1, M2, M3, M4, M8), the total cavity dispersion was estimated to be around -4440 fs².

To have a sufficient fluence for saturating the SWCNT-SA, two curved mirrors (M15 and M16), each with a radius of curvature (ROC) of 50 cm, were used to produce an estimated beam waist of 97 μm at the location of the saturable absorber.

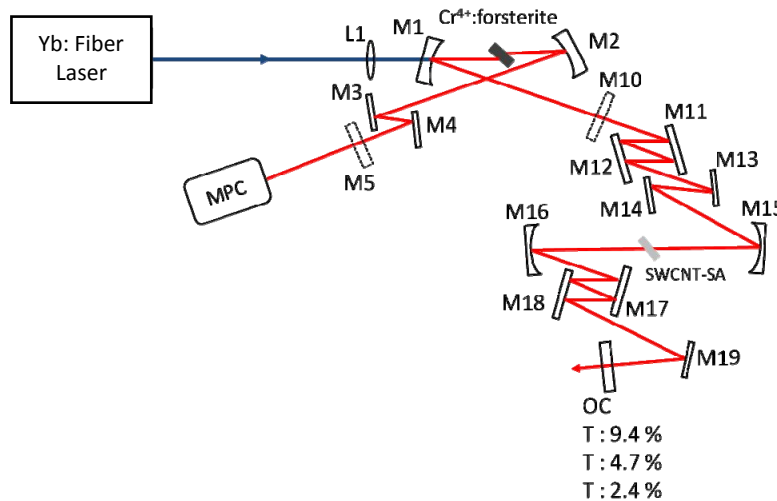


Figure 1. Schematic of the experimental set-up including the x-cavity, dispersion compensation optics (M11, M12, M13, M14, M17, M18, and M19), and the multi pass cavity (MPC).

2.2 Multipass-cavity (MPC) extension and CW operation of the Cr⁴⁺:forsterite laser

In order to scale the pulse energy, the overall optical path length was extended by incorporating a q-preserving MPC into the laser cavity [10]. The highly reflecting end mirror M5 of the x-cavity was removed and two flat folding DCM mirrors (M3 and M4) were used for adjusting the inclination angle and the input height of the beam entering the MPC. As seen in Fig. 2, the MPC contained a curved mirror (M6) with ROC = 4 m and a flat mirror (M7). The optical path lengths between M6 and M7, and also between M7 and M9 were equal to 1.65 m, a calculated value that satisfies the q-preserving condition of the MPC [10]. Both of the MPC mirrors had notches to allow beam injection and extraction. The laser beam completed 9 round trips between M6 and M7, and the exiting beam was retro-reflected with a curved end mirror (M9) with ROC = 2 m. In total, the MPC added an effective optical path length of 59.4 m to the original cavity, increasing the total cavity length to 66.5 m and reducing the pulse repetition frequency from 144 MHz to 4.51 MHz.

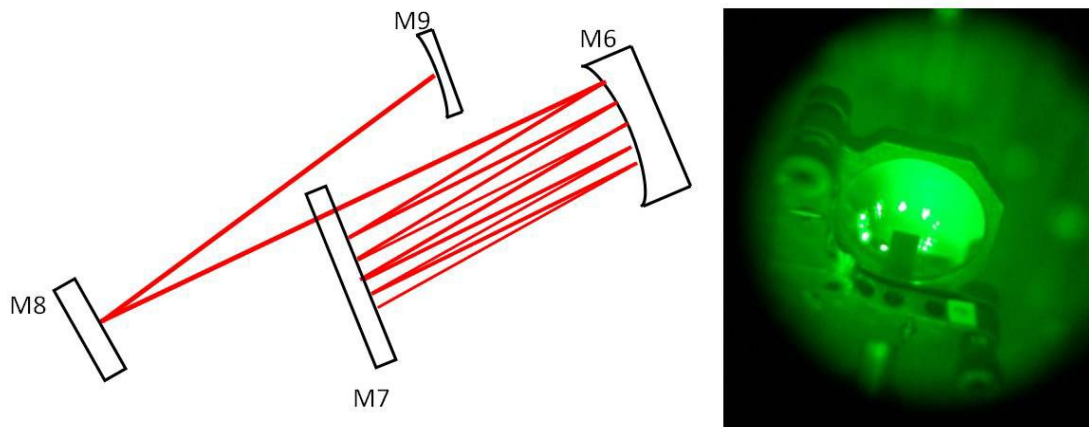


Figure 2. The MPC extension part of the Cr⁴⁺:forsterite laser. The photograph was taken with an infrared viewing camera and shows the circular spot pattern on the flat MPC mirror M7.

With the addition of the MPC and the dispersion compensation optics, a CW output power of 625 mW was obtained using a 4.7 % output coupler at 8 W of pump power. Fig. 3 shows the CW power performance of the Cr⁴⁺:forsterite laser for different laser architectures with the 4.7 % output coupler. After introducing the SWCNT-SA into the laser cavity, the efficiency of the laser decreased due to the additional loss originating from the saturable absorber.

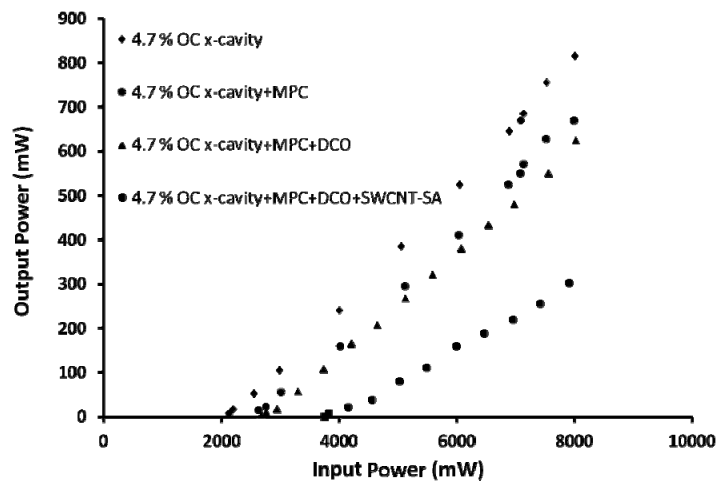


Figure 3. Power efficiency data for different cavity configurations with the 4.7 % output coupler in CW regime.

The power performance of the Cr⁴⁺:forsterite laser was further characterized at 9.4 % and 2.4 % output coupling. In particular, the 4.7 % output coupler was used as a folding mirror instead of an end retro-reflector to increase the effective output coupling of the cavity to 9.4 %. In this configuration, 495 mW of total average output power was obtained in the CW regime at 8 W of pump power. The CW output power was reduced compared to the case with 4.7 % output coupling, since 4.7 % output coupling is closer to the optimum output coupler value of the cavity. However, this configuration gives a higher extracavity/intracavity energy ratio so that higher pulse energy can be extracted from the laser during mode-locked operation for the same intracavity pulse energy. Figure 4 shows the CW power efficiency curves of the Cr⁴⁺:forsterite laser with the 9.4 % and 2.4 % output couplers.

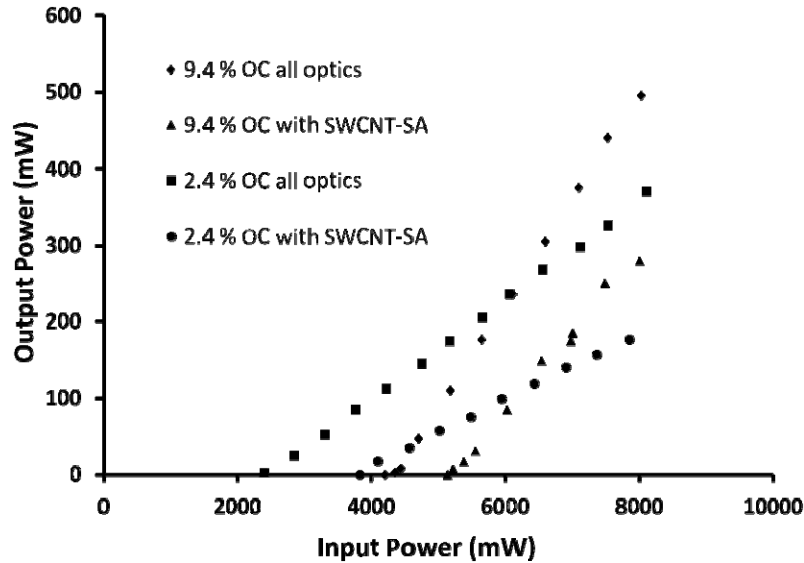


Figure 4. Power efficiency data for the composite laser cavity with 9.4 % and 2.4 % output couplers in CW regime. The data for the 9.4% output coupler is the total output power in two beams.

The double-pass optical loss of the SWCNT-SA was determined by measuring the threshold pump powers for different configurations and by using the equations [12]

$$(P_p)_{th} = A(L + T) \text{ and} \tag{1}$$

$$\frac{(P_p)_{th1}}{(P_p)_{th2}} = \frac{L_1 + T_1}{L_2 + T_2} \tag{2}$$

Above, $(P_p)_{th1,2}$ is the threshold pump power for the corresponding configuration (1 or 2), A is a constant, $L_{1,2}$ is the overall round-trip loss of the optical components and similarly $T_{1,2}$ is the transmission of the output coupler. Configurations 1 and 2 correspond to the cases without and with the SWCNT-SA in the cavity, respectively. Therefore, L_2 is given by

$$L_2 = L_1 + L_{SWCNT} \tag{3}$$

With the 9.4 % output coupler, the double-pass optical loss of the SWCNT-SA was found to be 3.76 % from the CW power efficiency data. This optical loss is approximately the sum of saturable and non-saturable losses and it is further reduced when the laser was mode-locked.

3. MODE-LOCKING RESULTS

The SWCNTs were synthesized by using the high-pressure CO conversion technique (HiPCO). SWCNTs were mixed with polymethylmethacrylate (PMMA) and the mixture was deposited on an optically polished 1-mm-thick quartz substrate. The relaxation time of the SWCNT-SA was less than 2 ps. The saturation fluence and the modulation depth were $10 \mu\text{J} / \text{cm}^2$ and 0.5 %, respectively [1]. The SWCNT-SA was placed at the location of the intracavity beam waist that had a radius of $97 \mu\text{m}$ as described above. When the laser was mode-locked with the 9.4% output coupler, stable single pulse operation was achieved with 46 mW of average output power. The corresponding incident fluence on the SWCNT-SA was determined to be $368 \mu\text{J}/\text{cm}^2$. The composite cavity was operated with three different output couplers (2.4 %, 4.7 % and 9.4 %). For an output coupler with a transmission larger than 11 %, the laser could not be operated at room temperature. Figures 5a-c show mode-locked spectra and autocorrelation traces for the three different output couplers and Table 1 lists the mode-locking results.

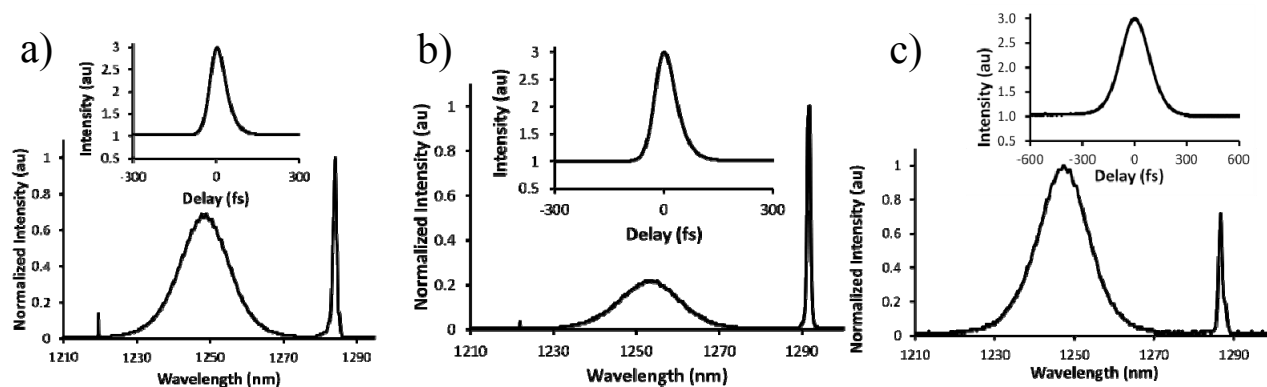


Figure 5. Mode-locked spectra and autocorrelation traces of the SWCNT-SA mode-locked Cr^{4+} :forsterite laser obtained with (a) 2.4 %, (b) 4.7 %, and (c) 9.4 % output couplers. The narrow peak around 1290 nm is believed to be due to GDD oscillations of the GTI mirrors.

Table 1. Mode locking results obtained with the SWCNT-SA mode locked Cr^{4+} :forsterite laser by using 2.4%, 4.7%, and 9.4% output couplers.

Output coupler transmission	Mode-locked power	Pulse energy	Peak power of the pulse	Center wavelength	Spectral width	Pulse duration	Time-bandwidth product
2.4 %	16 mW	3.54 nJ	29.5 kW	1248 nm	15.9 nm	120 fs	0.36
4.7 %	26 mW	5.76 nJ	46 kW	1253 nm	15.9 nm	124 fs	0.37
9.4 %	46 mW	10 nJ	84 kW	1247 nm	16 nm	121 fs	0.37

As a result, a multipass-cavity Cr^{4+} :forsterite laser operating at room temperature was successfully mode-locked by using a SWCNT-SA. The corresponding time-bandwidth products suggest that for all the output couplers used, the resulting pulses were nearly transform limited, assuming a sech^2 intensity profile.

4. DISCUSSION

Further increase of the pump power to generate pulses with higher energies caused temporal and spectral instabilities such as multi-pulsing or CW peaks in the spectrum. To explore the limiting factors for further energy scaling, a detailed analysis on critical power for the laser and nonlinear refractive index of the crystal were done. For a given pulse duration (τ_p), the net intracavity dispersion ($D = -4440 \text{ fs}^2$), and intracavity pulse energy (W), the net nonlinear coefficient (γ) due to the Cr^{4+} :forsterite crystal was calculated based on the soliton-area theorem [13].

$$W\tau = \frac{4|D|}{\gamma}, \quad (4)$$

where, γ is the nonlinear coefficient of the propagation medium and τ is equal to $\tau_p/1.76$. For nonlinear refractive index calculations, the nonlinearity due to air was neglected. Although the MPC introduces a long optical path in air, the nonlinearity of air at 1250 nm is negligible compared to the nonlinearity due to the Cr⁴⁺:forsterite crystal [14]. Therefore, γ was taken as the nonlinear coefficient associated with the Cr⁴⁺:forsterite crystal only. The nonlinear coefficient and the nonlinear refractive index (n_2) of the gain crystal are related through

$$\gamma = \frac{2\pi}{\lambda} n_2 \frac{2l_g}{A_{eff}^g}. \quad (5)$$

In Eq. 5, λ is the operation wavelength, l_g is the length of the gain medium and A_{eff}^g is the effective area of the beam inside the gain medium. The nonlinear refractive index of the gain medium was used to find the critical intracavity power P_{cr} for self focusing. P_{cr} is further related to the peak power at which pulsing instabilities begin to occur due to self-focusing effects inside the crystal. P_{cr} is given by [15]

$$P_{cr} = \frac{\alpha\lambda^2}{8\pi n_0 n_2}, \quad (5)$$

where, α is a dimensionless factor which was taken as 3.77 and n_0 is the linear refractive index of the Cr⁴⁺:forsterite crystal (1.635). Table 2 shows the calculated values of the critical power and the corresponding maximum peak power obtained for three different output couplers.

Table 2. Calculated values of the critical power and nonlinear refractive index for the SWCNT-SA mode locked Cr⁴⁺:forsterite laser for three different output couplers. The net intracavity dispersion was assumed to be -4440 fs².

Output coupler transmission	Intracavity energy	Pulse duration	Center wavelength	Nonlinear refractive index n_2	Critical power P_{cr}	Measured Intracavity power
2.4 %	147.5 nJ	120 fs	1248 nm	$6.81 \times 10^{-20} \text{ m}^2/\text{W}$	2 MW	1.2 MW
4.7 %	122.5 nJ	124 fs	1253 nm	$8 \times 10^{-20} \text{ m}^2/\text{W}$	1.8 MW	0.9 MW
9.4 %	108.5 nJ	121 fs	1247 nm	$9.36 \times 10^{-20} \text{ m}^2/\text{W}$	1.5 MW	0.9 MW

By neglecting the air nonlinearity and by using the soliton-area theorem, our calculated values for the nonlinear refractive index of the Cr⁴⁺: forsterite crystal are in reasonable agreement with the previously reported value of $6 \pm 4 \times 10^{-20} \text{ m}^2/\text{W}$ [16]. From Table 2, it can be clearly seen that, the only limiting factor for further energy scaling was the self-focusing induced nonlinearities of the gain medium.

5. CONCLUSIONS

In conclusion, we explored the energy scaling capability of SWCNT-SAs inside a multipass-cavity Cr⁴⁺:forsterite laser operated near 1250 nm. The SWCNT-SA was placed at a second beam waist formed by two curved mirrors, each with a radius of curvature of 50 cm. Together with the MPC and dispersion compensation optics, a total optical path length of 66.5 meters was obtained, corresponding to a repetition rate of 4.51 MHz. With the addition of DCMs and GTI mirrors, -4440 fs² net intracavity dispersion was achieved and the mode-locked laser produced nearly transform-limited pulses with all output couplers used. With the 9.4% output coupler, The SWCNT-SA mode-locked Cr⁴⁺:forsterite laser produced nearly transform-limited solitary pulses with a pulse energy of around 10 nJ and peak power of 84 kW. The pulse duration and spectral width (FWHM) were 121 fs and 16 nm, respectively, resulting in a time-bandwidth product

of 0.37. To the best of our knowledge, 84 kW is the highest peak power generated to date for a femtosecond solid-state laser mode-locked with a SWCNT-SA.

For further investigation of energy scaling, the composite cavity was operated with three different output couplers (2.4 %, 4.7 % and 9.4 %). By using the soliton-area theorem, the nonlinear refractive index of the Cr⁴⁺:forsterite crystal was determined for each case. The resulting value was in good agreement with the previously reported nonlinear refractive index value. It was shown that the only limitation which prevents further increase in the peak power was due to self-focusing based pulsing instabilities. Hence, SWCNT-SAs have the potential to be used for the mode-locking of high-power lasers based on different types of gain media.

REFERENCES

- [1] Cho, W. B., Yim, J. H., Choi, S. Y., Lee, S., Schmidt, A., Steinmeyer, G., Griebner, U., Petrov, V., Yeom, D. I., Kim, K. and Rotermund, F., "Carbon Nanotubes: Boosting the non linear optical response of carbon nanotube saturable absorbers for broadband mode-locking of bulk lasers", *Adv. Funct. Mater.*, 20 (12), 1937-1943 (2010).
- [2] Baek, I. H., Choi, S. Y., Lee, H. W., Cho, W. B., Petrov, V., Agnesi, A., Pasiskevicius, V., Yeom, D. I., Kim, K. and Rotermund, F., "Single-walled carbon nanotube saturable absorber assisted high-power mode-locking of a Ti:sapphire laser", *Opt. Express* 19 (8), 7833-7838 (2011).
- [3] Cho, W. B., Yim, J. H., Choi, S. Y., Lee, S., Griebner, U., Petrov, V. and Rotermund, F., "Mode-locked self-starting Cr:forsterite laser using a single-walled carbon nanotube saturable absorber", *Opt. Lett.* 33 (21), 2449-2451 (2008).
- [4] Schmidt, A., Koopmann, P., Huber, G., Fuhrberg, P., Choi, S. Y., Yeom, D. I., Rotermund, F., Petrov, V. and Griebner, U., "175 fs Tm:Lu₂O₃ laser at 2.07 μ m mode-locked using single-walled carbon nanotubes", *Opt. Express* 20 (5), 5313-5318 (2012).
- [5] Avouris, P., Freitag, M. and Perebeinos, V., "Carbon-nanotube photonics and optoelectronics" *Nat. Photonics* 2 (6), 341-350 (2008).
- [6] Bachilo, S. M., Strano, M. S., Kittrell, C., Hauge, R. H., Smalley, R. E. and Weisman, R. B., "Structure-assigned optical spectra of single-walled carbon nanotubes", *Science* 298 (5602), 2361-2366 (2002).
- [7] Stoneman, R. C., "Eye safe rare earth solid-state lasers," in [Solid State Lasers and Applications], A. Sennaroglu, ed. (CRC Press).
- [8] Liu, T. M., Chu, S. W., Sun, C. K., Lin, B. L., Cheng, P. C. and Johnson, I., "Multiphoton confocal microscopy using a femtosecond Cr:forsterite laser", *Scanning* 23 (4), 249-254 (2001).
- [9] Tearney, G. J., Brezinski, M. E., Bouma, B. E., Boppart, S. A., Pitris, C., Southern, J. F. and Fujimoto, J. G., "In vivo endoscopic optical biopsy with optical coherence tomography", *Science* 276 (5321), 2037-2039 (1997).
- [10] Sennaroglu, A., Kowalewicz, A. M., Ippen, E. P. and Fujimoto, J. G., "Compact femtosecond lasers based on novel multi-pass cavities", *IEEE J. Quantum Electron.* 40 (5), 519-528 (2004).
- [11] Baylam, I., Ozharar, S., Cankaya, H., Choi, S. Y., Kim, K., Rotermund, F., Griebner, U., Petrov, V. and Sennaroglu, A., "Energy scaling of a carbon nanotube saturable absorber mode-locked femtosecond bulk laser", *Opt. Lett.* 37 (17), 3555-3557 (2012).
- [12] Sennaroglu, A., [Photonics and laser engineering : principles, devices, and applications] McGraw-Hill, New York, 368 (2010).
- [13] Haus, H. A., "Mode-locking of lasers", *IEEE J. of Sel. Top. in Quantum Electron.* 6 (6), 1173-1185 (2000).
- [14] Fedorov, V. Y. and Kandidov, V. P., "A nonlinear optical model of an air medium in the problem of filamentation of femtosecond laser pulses of different wavelengths", *Opt. Spectrosc.* 105 (2), 280-287 (2008).
- [15] Huang, D., Ulman, M., Acioli, L. H., Haus, H. A. and Fujimoto, J. G., "Self-focusing-induced saturable loss for laser mode-locking", *Opt. Lett.* 17 (7), 511-513 (1992).
- [16] Chassagne, B., Ivanov, A., Oberle, J., Jonusauskas, G. and Rulliere, C., "Experimental determination of the nonlinear refractive index in an operating Cr:forsterite femtosecond laser", *Opt. Commun.* 141 (1-2), 69-74 (1997).